Journal of Alloys and Compounds 550 (2013) 479–482

Contents lists available at SciVerse ScienceDirect

Journal of Alloys and Compounds

journal homepage: www.elsevier.com/locate/jalcom

Effects of S on solid solubility of Ag and electrical properties of Ag-doped ZnO films grown by radio frequency magnetron sputtering

J.C. Li [a], Y.F. Li [a], T. Yang [a], B. Yao [a,*], Z.H. Ding [a], Y. Xu [a], Z.Z. Zhang [b], L.G. Zhang [b], H.F. Zhao [b], D.Z. Shen [b]

[a] State Key Laboratory of Superhard Materials and College of Physics, Jilin University, Changchun 130023, PR China
[b] Key Laboratory of Excited State Processes, Chinese Academy of Sciences, Changchun Institute of Optics Fine Mechanics and Physics, Chinese Academy of Sciences, Changchun 130033, PR China

ARTICLE INFO

Article history:
Received 8 October 2012
Accepted 24 October 2012
Available online 2 November 2012

Keywords:
ZnO films
Ag
S
Solid solubility
Doping

ABSTRACT

Effects of S on solid solubility of Ag and electrical properties of Ag-doped ZnO films are investigated by experimental and first-principles studies. It is found that S alloying in ZnO can increase solid solubility of Ag substituting for Zn (Ag_{Zn}) due to that Ag binds more easily with S than O, leading to that Ag–S codoped ZnO films gradually transform from n- to p-type conductivity with increasing S content. The low-temperature photoluminescence measurement and first-principles calculation indicate that there are two kinds of Ag_{Zn} and Ag_{Zn}–nS_O acceptors in the p-type Ag–S codoped ZnO and the Ag_{Zn}–nS_O acceptor has lower formation energy and acceptor transition energy than Ag_{Zn}. The p-type conduction of the Ag–S codoped ZnO comes dominantly from contribution of the Ag_{Zn}–nS_O acceptor.

1. Introduction

Zinc oxide (ZnO) exhibits attractive properties such as a direct wide band gap of 3.37 eV and a high excitonic binding energy of 60 meV at room temperature that can be exploited in a number of applications of semiconductor and optoelectronic devices [1,2]. However, the realization of any practically useful device has been limited by the lack of stable, reproducible p-type ZnO. Based on simple valence electron arguments, a great deal of effort has been devoted to fabricate p-type ZnO by doping group I (Li [3] and Na [4]) and V elements (N [5], P [6], As [7] and Sb [8]), but it is proven that it is difficult to achieve p-type doping by these elements, and the obstacle is usually recognized as caused by the following problems: low acceptor solubility, high ionization energy of the acceptors, and various self-compensating complexes. For instance, Li, with small ionic radius, tends to occupy the interstitial site (denoted as Li_i) rather than substitutional site (denoted as Li_{Zn}) in ZnO lattice. Although Li_{Zn} is a shallow acceptor, Li exists mainly in the form of Li_i and acts as donor in ZnO [9,10], resulting in compensation of Li_i for Li_{Zn} and n-type conduction or electric insulation of the Li-doped ZnO. Among the group V elements, N is controversially accepted as the most likely candidate for p-type doping in ZnO due to similarities in radii and electronic structure of N and O [11]. However, since thermodynamic solubility of N in ZnO is zero and N acceptor level is deep [12] as well as self-compensating caused by $(N_2)_O$ [13], the N-doped ZnO with stable p-type conductivity is usually prepared difficultly, and it often transforms into n-type conductivity after several days. Obviously, if we want to realize p-type doping in ZnO, it is necessary to resolve successfully the problems above.

The drive for ZnO based optoelectronic devices gives rise to intense focus on group-IB elements. Recently, Yan et al. [14] presented that the formation energies of group-IB (Ag, Cu, and Au) elements at the substitutional site are much lower than those at the interstitial sites, which can reduce the formation of interstitial donors and alleviate the self-compensation issue. However, they also suggested that the ionization energy of IB group element is usually quite large, for example, the ionization energy of Ag_{Zn}^{1+} acceptor is about 0.4 eV, which is too large to realize p-type conduction of Ag-doped ZnO. Recently, Persson et al. [15] revealed that the substitution of sulfur anion at oxygen sites in ZnO creates electronic state in the forbidden gap and shows strong valence band offset bowing due to overlapping of Zn–S like bonds on ZnO. The strong VB-offset bowing can be utilized to reduce the acceptor level, such as Ag_{Zn}^{1+} acceptor, furthermore, it is well known that melting point of Ag_2S (825 °C) [16] is higher than that of Ag_2O (280 °C) [17], suggesting that Ag_2S is more stable than Ag_2O under annealing, that is, S alloying in ZnO may increase the solid solubility of Ag. In our previous work, the stable Cu–S codoping p-type ZnO with a hole concentration of $\sim 10^{19}$ has been obtained [18], demonstrating that S alloying in ZnO may be helpful to overcome the low solid solubility and high acceptor ionization energy of Ag_{Zn} in ZnO.

* Corresponding author. Tel.: +86 43186176355.
E-mail addresses: phys.yao@yahoo.cn, binyao@jlu.edu.cn (B. Yao).

0925-8388/$ - see front matter © 2012 Elsevier B.V. All rights reserved.
http://dx.doi.org/10.1016/j.jallcom.2012.10.103

In the present work, the Ag–S codoped ZnO films were prepared on quartz substrates by radio frequency (RF) magnetron sputtering. The S contents in ZnO were tuned by means of changing substrate temperature. Effects of S on solid solubility of Ag and electrical properties of Ag-doped ZnO films were investigated by combining experiment with first-principles calculation.

2. Experimental details

The Ag–S codoped ZnO thin films were grown on quartz substrates by radio frequency (RF) magnetron sputtering. For obtaining ZnO:(Ag, S) films, the ZnS thin wafers with Ag wires on their surface were putted on the ZnO ceramic target. The device structure is simply schematically shown in Fig. 1. Before deposition, the vacuum chamber was evacuated to a base pressure of 5×10^{-4} Pa and then filled with mixture of Ar (38 SCCM) and O_2 (2 SCCM) to 1.0 Pa, which is kept during depositing process. The ZnO:(Ag, S) films were deposited at 200, 350 and 500 °C, denoted as samples A, B and C, respectively. For comparison, an undoped ZnO film (denoted as sample D) was fabricated at 500 °C by using a high purity ZnO target. All as-grown films show high resistivity, for improving the electrical properties, they were annealed at 600 °C under 3×10^{-3} Pa for 15 min. The structures of the films were characterized by X-ray diffraction (XRD) with Cu $K_{\alpha 1}$ radiation ($\lambda = 0.15406$ nm). The electrical properties were measured with the van der Pauw configuration by a Hall Effect measurement system (Lakershore HMS 7707) at room temperature. The composition of the films was detected by using energy dispersive X-ray spectroscopy (EDS). The low-temperature photoluminescence (PL) measurement were performed by using the UV Labran Infinity Spectrophotometer with He-Cd laser line of 325 nm as an excitation source.

3. Results and discussion

Fig. 2 shows the XRD patterns of the undoped and Ag–S codoped ZnO films annealed at 600 °C. The (002) diffraction peak of the annealed undoped ZnO (sample D) locates at 34.43°. The *c*-axis lattice constant of the annealed ZnO is calculated to be 0.5205 nm, which is very close to 0.5209 nm of bulk ZnO. For the sample A, only XRD peaks of wurtzite ZnO are observed, which are corresponding to the (002), (103) and (004) diffractions, respectively. However, an additional peak located at 38.06° (marked as ■) is observed in both sample B and C besides the XRD peaks of the wurtzite ZnO, which is ascribed to diffraction of (111) plane of metal Ag, implying that some Ag doped in ZnO precipitate from ZnO in a form of metal Ag. It is noted that the (002) diffraction peak of the sample A locates at 34.39°, which is smaller than 34.43° of the undoped ZnO. The smaller diffraction angle of the sample A originates from the Ag and S doping because ionic radius of Ag^{1+} and S^{2-} is larger than that of Zn^{2+} and O^{2-}, respectively. This suggests that Ag and S may substitute Zn and O sites in sample A. However, the (002) peak positions of the annealed sample B and C locate at 34.44° and 34.45°, respectively, which are almost the same as 34.43° of the annealed undoped ZnO, implying that contents of Ag and S substituting Zn and O are a little in the sample B and C.

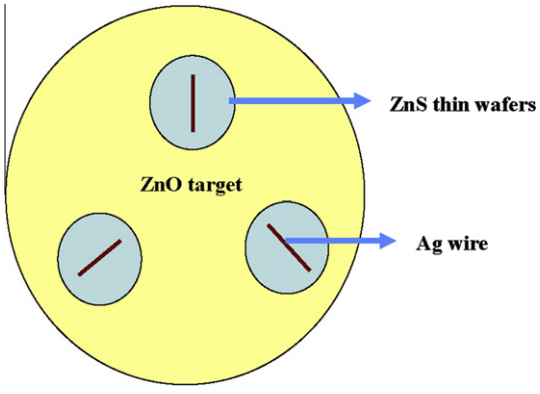

Fig. 1. Schematic diagram of the sputtered targets.

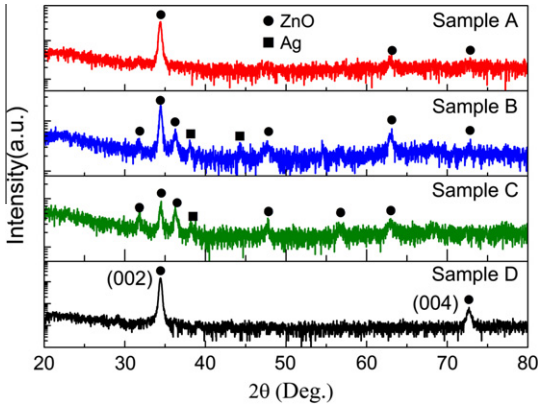

Fig. 2. XRD patterns of the annealed Ag–S codoping and undoped ZnO thin films.

To determine content of Ag and S in the annealed sample A, B and C, EDS measurement were performed and plotted as a function of substrate temperature, as shown in Fig. 3. The Ag contents are 2.3%, 2.7% and 2.5% for sample A, B and C, respectively. The Ag content are somewhat larger in both sample B and C than in sample A, and the variation rates of Ag content of sample B and C with respect to sample A are 17% and 9%, respectively, as shown in the inset of Fig. 3. In contrast, the S contents significantly decreases from 1.54% to 0.45% as the substrate temperature increases from 200 to 500 °C, that is, the S content is larger in the sample A than in the sample B and C. The variation rates of S contents of sample B and C with respect to sample A are 51% and 71%, as shown in the inset of Fig. 3. It should be noted that the diffraction peaks of metal Ag are observed in the annealed sample B and C, but not in the annealed sample A, and (002) peak positions of the annealed sample B and C are almost the same as the annealed undoped ZnO, while the (002) peak position of the sample is lower than that of the undoped ZnO. These results imply that the Ag almost exists in the form of metal Ag in the annealed sample B and C but not in the form of substitutional Ag_{Zn}. As a result, the content of Ag_{Zn} in the annealed sample A is larger than the annealed sample B and C. Based on the analysis above, it is deduced that the Ag_{Zn} content in the ZnO decreases with decreasing S content, or accordingly, Ag_{Zn} solubility increases with increasing S content in ZnO. According to Hard-Soft Acid–Base theory (HSAB) [19,20], Ag reacts more easily with S than O, and Ag_2S is more stable than Ag_2O, that means that the S doping into ZnO and occupying O site prefers to bind

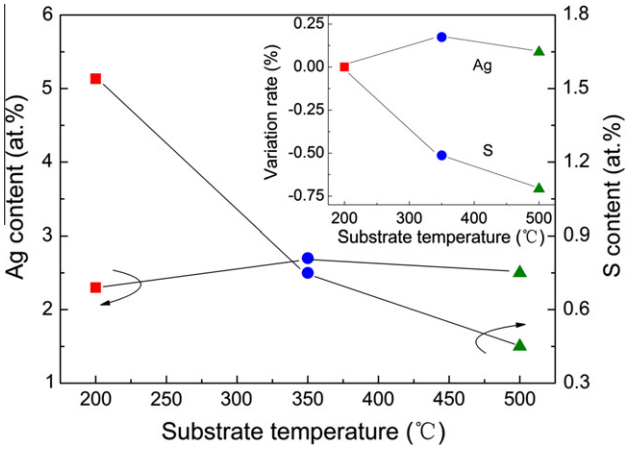

Fig. 3. The contents of Ag and S as a function of substrate temperature. The inset shows the variation rate of Ag and S contents in the samples B and C with respect to the sample A, respectively.

Table 1
The electrical properties of the annealed Ag–S codoped and undoped ZnO thin films.

Sample	S content (%)	Ag content (%)	Substrate temp. (°C)	Resistivity (Ω cm)	Carrier density (cm^{-3})	Mobility ($cm^2 V^{-1} s^{-1}$)	Type
A	1.54	2.3	200	3.36×10^3	3.33×10^{15}	0.56	p
B	0.75	2.7	350	83.0	1.75×10^{17}	0.29	n
C	0.45	2.5	500	8.35	2.06×10^{17}	3.67	n
D	0	0	500	0.39	2.36×10^{18}	6.68	n

with Ag_{Zn} to form Ag_{Zn}–S_O bond, and the Ag_{Zn} in the Ag_{Zn}–S_O bond is more stable than one in the Ag_{Zn}–O bond. Therefore, incorporation of S can enhance stability of Ag_{Zn} acceptor and solubility of Ag_{Zn} in ZnO.

Table 1 lists the electrical properties of all the annealed samples. The annealed sample A with high S content shows p-type conductivity with a resistivity of $3.36 \times 10^3\ \Omega$ cm, a hole concentration of $3.33 \times 10^{15}\ cm^{-3}$, a mobility of $0.56\ cm^2\ V^{-1}\ s^{-1}$. However, both samples B and C with low S content show n-type conduction. From samples B to D, the resistivity decreases, but the electron concentration and mobility increases. It is known from Fig. 3 that the contents of Ag_{Zn} and S decreases from sample A to C. Combining with Table 1 results, it is found that, with decreasing Ag_{Zn} content, the conducting type of the Ag–S codoped ZnO changes from p- to n-type, the resistivity decrease but the carrier concentration and mobility increases, implying that the conductivity of the annealed Ag–S codoped ZnO is related to contents of Ag_{Zn}. For the sample A, it has more Ag_{Zn} acceptor defects, and the amount of the Ag_{Zn} acceptor is larger than that of native donor defects, leading to p-type conduction. However, for the sample B and C, the Ag_{Zn} content decreases with respect to the sample A, which results in that the amount of Ag_{Zn} acceptor is less than that of native donor defects, hence the sample B and C show n-type conduction. Since Ag_{Zn} content decreases from sample A to C, the compensation of Ag_{Zn} acceptor for native donors decreases but crystal quality increases, which should make resistivity decrease and electron concentration increase, in agreement with results in Table 1.

In order to understand further the origin of p-type conductivity, low temperature (91 K) photoluminescence (PL) measurement are performed for the annealed sample A and B, as shown in Fig. 4. The sample B consists of three emission peaks located at 3.360, 3.319 and 3.249 eV. The peak at 3.360 eV can be assigned a neutral donor bound exciton transition (D°X) [21,22]. The peak at 3.319 eV can be due to a neutral acceptor bound exciton transition (A°X) related to Ag_{Zn} acceptor [21]. The deep acceptor bound exciton was also reported elsewhere. Look et al. [23] and Ryu et al. [24] observed the A°X of N- and As-doped ZnO located at 3.315 eV at 2 K and 3.32 eV at 20 K, respectively. Moreover, it can be found from PL that a small number of Ag_{Zn} acceptors still exist in the sample B due to the appearance of A°X. However, although a small number of Ag_{Zn} acceptors exist in the sample B, the D°X dominates in PL, implying that the donors are still dominant in sample B, therefore, the sample B still shows n-type conductivity. The peak at 3.249 eV exhibits a longitudinal optical (LO) phonon replica of A°X separated by approximate 72 meV, therefore, it is attributed to A°X-LO. By using the Gaussian fitting method, the PL of the sample A reveals four peaks located at 3.370, 3.331, 3.312 and 3.240 eV, respectively, as shown in the inset of Fig. 4. The peak at 3.370 eV can be assigned to a free exciton (FX) emission [22]. The appearance of FX suggests the annealed sample A has high crystallization quality. The new peak at 3.331 eV can be ascribed to a new neutral acceptor bound exciton (new-A°X) corresponding to Ag_{Zn}–nS_O complex acceptor [22], implying that the sample A exists a large number of Ag–S bonds, which can stabilize the Ag_{Zn} acceptor at Zn site under post-annealing, leading to p-type conduction of the

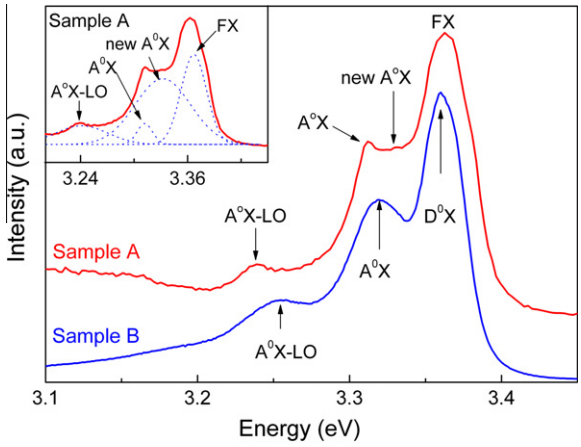

Fig. 4. 91 K PL spectra of the annealed Ag–S codoped ZnO deposited at 200 (sample A) and 350 °C (sample B). The inset shows the fitting PL spectrum of the sample A.

sample A. In contrast, the peak related to Ag_{Zn}–nS_O complex acceptor does not be observed in the sample B. This is because most of Ag_{Zn} acceptors escape from Zn sites and form metal Ag due to low S content in the sample B. The peak at 3.312 and 3.240 eV can be considered as recombination of A°X related to Ag_{Zn} acceptor and A°X-LO, respectively. They show slightly red shift compared to that of sample B, which may be due to that the larger S content in sample A leads to the larger VB-offset bowing.

The ionization energy E_A of the two acceptors of Ag_{Zn} and Ag_{Zn}–nS_O in sample A are estimated by Haynes rule [25],

$$E_b = \alpha E_A \quad (1)$$

where E_b is the exciton localization energy that can be obtained from the difference between the FX and the A°X, and α is a Haynes factor. Based on the low-temperature PL result of the sample A shown in Fig. 4, the E_b for Ag_{Zn} and Ag_{Zn}–nS_O acceptors is estimated to be 58 and 39 meV, respectively. Using the appropriate value $\alpha = 0.24$ [26], the ionization energy for Ag_{Zn} and Ag_{Zn}–nS_O acceptors is calculated to be about 242 and 163 meV, respectively. Obviously, incorporation of S can form the Ag_{Zn}–nS_O complex acceptor with ionization energy smaller than that of Ag_{Zn} acceptor, which favors p-type conductivity.

To understand better the experimental results, first-principles calculations were performed using the VASP code with the projector augmented wave (PAW) potentials for electronic interaction and generalized gradient approximation (GGA) for electron exchange and correlation [27,28]. For simulating the Ag and S codoping in ZnO, the wurtzite 72-atom $3 \times 3 \times 2$ supercells with the nearest neighbor (NN) Ag_{Zn}–nS_O complex were constructed. A $2 \times 2 \times 2$ k-point mesh was used for the Brillouin zone integration and a more refined $(8 \times 8 \times 8)$ k-point mesh was used for the density-of-states (DOS) calculations. In the calculations, all the atoms are allowed to relax until the Hellmann–Feynman forces acting on them become less than 0.01 eV/Å.

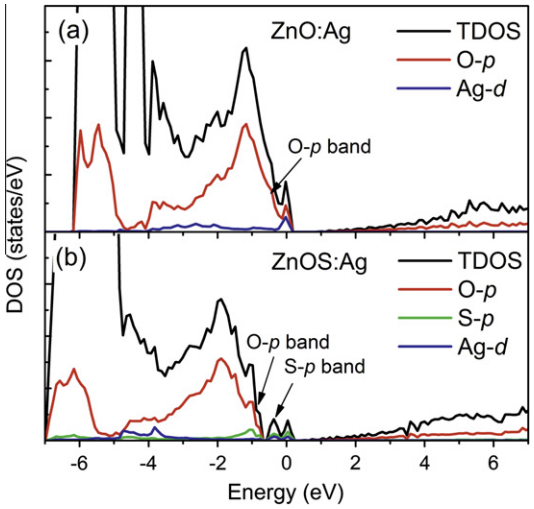

Fig. 5. First-principles calculated total and partial DOS of the 72-atom ZnO supercell with (a) Ag_{Zn} and (b) Ag_{Zn}–$4S_O$ complex within the GGA approximation.

We first calculated the binding energy of Ag_{Zn}–nS_O complex in ZnO in order to determine if Ag–nSo complex is stable. The binding energy can be expressed as follows,

$$E_b = E_{tot}(Ag_{Zn} + nS_O) + E_{tot}(ZnO) - E_{tot}(Ag_{Zn})E_{tot}(nS_O) \quad (2)$$

where E_{tot} is the total energy of the system calculated with the same supercell. A negative E_b indicates that the complex tends to bind to each other and forms a more stable structure. The calculated binding energy E_b for the complex is −0.8 and −1.3 eV for $n = 2$ and $n = 4$, respectively, indicating that the complex is stable with respect to the isolated Ag_{Zn} and S_O defects, which is in good agreement with experimental results.

To further understand the S induced decrease of acceptor ionization energy from PL spectrum, the acceptor transition energy, $\varepsilon(0/-)$, of Ag_{Zn}–nS_O complex was also calculated. The $\varepsilon(0/-)$ is 0.44 eV for the Ag_{Zn} in ZnO, close to the result calculated by Yan et al. [14]. As S and Ag codoped into ZnO, the obtained $\varepsilon(0/-)$ of Ag_{Zn}–nS_O complex is 0.26 and 0.18 eV for $n = 2$ and $n = 4$, respectively, well explaining the shallowing of acceptor level observed in the PL measurements. Fig. 5(a) and (b) show the calculated total and partial density of states (DOS) of the 72-atom ZnO supercells with Ag_{Zn} and Ag_{Zn}–$4S_O$ complex, respectively. For the ZnO supercell with Ag_{Zn}, the valence band maximum (VBM) is composed of O-2p bands. For the ZnO supercell with Ag_{Zn}–$4S_O$ complex, S-3p bands occur above O-2p band, suggesting the VBM level is equivalently pushed to higher energy, which leads to lower acceptor transition energy. Therefore, this result well supports the acceptor shallowing observed in the PL measurements.

4. Conclusions

In summary, our experimental and first-principles studies indicate that S codoping to ZnO with Ag can enhance the solubility of Ag_{Zn} acceptor and form the shallower Ag_{Zn}–nS_O complex than Ag_{Zn}. Furthermore, the p-type conduction was observed in Ag–S codoped ZnO. These results indicate that Ag–S codoping may be a promising method for the realization of p-type ZnO.

Acknowledgments

This work was supported by the National Natural Science Foundation of China under Grant Nos. 10874178, 11074093, 61205038 and 11274135, Natural Science Foundation of Jilin province under Grant No. 201115013, and National Fund for Fostering Talents of Basic Science under Grant No. J1103202.

References

[1] D.C. Look, D.C. Reynolds, J.W. Hemsky, R.L. Jones, J.R. Sizelove, Appl. Phys. Lett. 75 (1999) 811.
[2] Z.K. Tang, G.K.L. Wong, P. Yu, M. Kawasaki, A. Ohtomo, H. Koinuma, Y. Segawa, Appl. Phys. Lett. 72 (1998) 3270.
[3] J.G. Lu, Y.Z. Zhang, Z.Z. Ye, Y.J. Zeng, H.P. He, L.P. Zhu, J.Y. Huang, L. Wang, J. Yuan, B.H. Zhao, X.H. Li, Appl. Phys. Lett. 89 (2006) 112113.
[4] S.S. Lin, Appl. Phys. Lett. 101 (2012) 122109.
[5] M.A. Myers, M.T. Myers, M.J. General, J.H. Lee, L. Shao, H. Wang, Appl. Phys. Lett. 101 (2012) 112101.
[6] J.H. Lim, C.K. Kang, K.K. Kim, I.K. Park, D.K. Hwang, S.J. Park, Adv. Mater. 18 (2006) 2720.
[7] C.K. To, B. Yang, S.C. Su, C.C. Ling, C.D. Beling, S. Fung, J. Appl. Phys. 110 (2011) 11352.
[8] Z. Zhao, L. Hu, H. Zhang, J. Sun, J. Bian, J. Zhao, Appl. Surf. Sci. 257 (2011) 512.
[9] C.H. Park, S.B. Zhang, Su-Huai Wei, Phys. Rev. B 66 (2002) 073202.
[10] D.C. Look, R.L. Jones, J.R. Sizelove, N.Y. Garces, N.C. Giles, L.E. Halliburton, Phys. Status Solidi A 195 (2003) 171.
[11] A. Kobayashi, O.F. Sankey, J.D. Dow, Phys. Rev. B 28 (1983) 946.
[12] J.L. Lyons, A. Janotti, C.G. Van de Walle, Appl. Phys. Lett. 95 (2009) 252105.
[13] X.Y. Chen, Z.Z. Zhang, B. Yao, M.M. Jiang, S.P. Wang, B.H. Li, C.X. Shan, L. Liu, D.X. Zhao, D.Z. Shen, Appl. Phys. Lett. 99 (2009) 091908.
[14] Y.F. Yan, M.M. Al-Jassim, Su-Huai Wei, Appl. Phys. Lett. 89 (2006) 181912.
[15] C. Persson, C. Platzer-Björkman, J. Malmström, T. Törndahl, M. Edoff, Phys. Rev. Lett. 97 (2006) 146403.
[16] The melting point (decomposition) of Ag_2S is 825 °C, http://en.wikipedia.org/wiki/Silver_sulfide.
[17] The melting point (decomposition) of Ag_2O is 280 °C, http://en.wikipedia.org/wiki/Silver_oxide.
[18] H.L. Pan, B. Yao, T. Yang, Y. Xu, B.Y. Zhang, W.W. Liu, D.Z. Shen, Appl. Phys. Lett. 97 (2010) 142101.
[19] P.W. Ayers, Faraday Discuss. 135 (2007) 161–190.
[20] P.W. Ayers, R.G. Parr, R.G. Pearson, J. Chem. Phys. 124 (2006) 194107.
[21] L. Duan, W. Gao, R.Q. Chen, Z.X. Fu, Solid State Commun. 145 (2008) 479.
[22] L.J. Sun, J. Hu, H.Y. He, X.P. Wu, X.Q. Xu, B.X. Lin, Z.X. Fu, B.C. Pan, Solid State Commun. 149 (2009) 1663.
[23] D.C. Look, D.C. Reynolds, C.W. Litton, R.L. Jones, D.B. Eason, G. Cantwell, Appl. Phys. Lett. 81 (2002) 1830.
[24] Y.R. Ryu, S. Zhu, D.C. Look, J.M. Wrobel, H.M. Jeong, H.W. White, J. Cryst. Growth 216 (2000) 330.
[25] Y.R. Ryu, T.S. Lee, H.W. White, Appl. Phys. Lett. 83 (2003) 87.
[26] J. Gutowski, N. Presser, I. Broser, Phys. Rev. B 38 (1988) 9746.
[27] J.P. Perdew, K. Burke, M. Ernzerhof, Phys. Rev. Lett. 77 (1996) 3865.
[28] P.E. Blöchl, Phys. Rev. B 50 (1994) 17953.